Available online at www.sciencedirect.com
SCIENCE DIRECT®
ELSEVIER
International Journal of Thermal Sciences 42 (2003) 417–423
International Journal of Thermal Sciences
www.elsevier.com/locate/ijts

Numerical analysis and experimental validation of high pressure gas quenching

I. Elkatatny, Y. Morsi *, A.S. Blicblau, S. Das, E.D. Doyle

IRIS, Swinburne University of Technology, Hawthorn, Victoria 3122, Australia

Received 6 August 2001; accepted 3 June 2002

Abstract

Aided by the computational fluid dynamics package CFX-4 a transient flow model has been used to simulate the process of high pressure gas quenching of a large H13 die. The predicted temperature distributions, obtained under steady and transient flow conditions, together with experimental data have been compared, and a good agreement was obtained. This suggests that a steady state simulation can be effectively used in this type of study to achieve accurate simulated data with reduced computational time. This series of studies is seen as the precursor to the development of an overall simulation procedure for simultaneous distortion and heat transfer characterisation of the die leading to optimum heat treatment control.

Keywords: Simulation; Computational fluid dynamics; Heat treatment; Quenching; Vacuum; Die

1. Introduction

High pressure gas quenching is a form of heat treatment process used frequently in various industries such as the aerospace the automotive, machine tool and other advanced manufacturing processes. The use of gas quenching can significantly affect the mechanical and physical properties of a material, for obtaining near net shape of metal components. Although the purpose of this process is to improve the performance of components, degrading or destroying of products may occur if improper quenching processes are performed.

Heat treatment of large single metal components may cause a number of deficiencies and problems during the production of complex geometry products. Recently, however with the availability of progressive faster and more powerful computers it is now possible for numerical modelling to simulate heat treatment processes including gas quenching in a vacuum heat treatment furnace. To date, many numerical schemes to simulate various heat treatment processes have been used to predict heat and fluid the flow characteristics within the furnace as well as the temperature distributions of the metallic components [1–6].

On recognizing the importance of using computational procedures for simulation of heat treatment processes, the authors and co-workers have developed a three-dimensional computational model to analyse the heat transfer and fluid flow phenomena in a high-pressure gas quenching vacuum furnace under steady state condition [7]. However, a transient flow model is believed to better represent the flow characteristics and heat transfer in high-pressure gas quenching furnaces. Two studies were carried out; a numerical simulation of the quenching and marquenching processes based on the steady state and transient flow behaviour developed inside a furnace hot zone during the quenching process, and experimental work to validate the numerical simulation.

2. Experimental set-up and procedure

The vacuum heat treatment furnace used in this work was an Abar Ipsen Tool Treater model VTTC-K-524. The working dimensions of the furnace are $750 \times 600 \times 900$ mm with a recommended load of up to 800 kg. A convection fan operating at 2 bar pressure of nitrogen provides a uniform heating up to 860 °C followed by radiant heating for temperatures up to 1315 °C.

Quenching is accomplished using nitrogen gas circulated through oscillating gas nozzles at the top and bottom of

* Corresponding author.
E-mail address: ymorsi@swin.edu.au (Y. Morsi).

1290-0729/02/$ – see front matter © 2002 Éditions scientifiques et médicales Elsevier SAS. All rights reserved.
doi:10.1016/S1290-0729(02)00042-X

Fig. 1. Photograph an H13 die block for vacuum heat treatment.

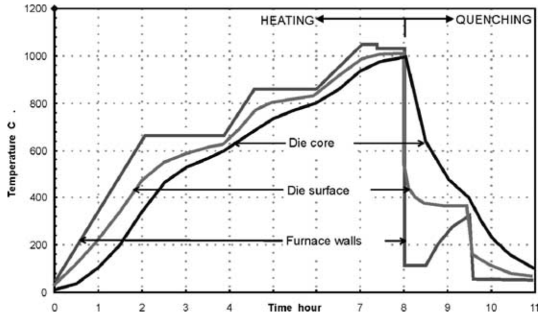

Fig. 2. Chart recording of the heating and marquenching cycle of the H13 die.

the furnace. The gas is diverted from the top to the bottom nozzles in every 20 seconds. Quenching pressure can be varied from 1 to 6 bars absolute. During quenching the recirculating gas is driven by a 200 HP fan through a large heat exchanger capable of maintaining the gas at a constant temperature of 20 °C and a velocity of 60 $m \cdot s^{-1}$ on entry into the hot zone.

A die made from H13 hot work tool steel, weighing 385 kg, was used for both the heat treatment and simulation processes. H13 tool steel is a versatile chromium-molybdenum hot work steel that is widely used in hot work and cold work tooling applications. The hot hardness (hot strength) of H13 resists thermal fatigue cracking which occurs as a result of cyclic heating and cooling cycles in hot work tooling applications. Because of its excellent combination of high toughness and resistance to thermal fatigue cracking (also known as heat checking) H13 is used for more hot work tooling applications than any other tool steel.

The die, as shown in Fig. 1, had been previously heat treated and used in service with overall dimensions of $360 \times 360 \times 560$ mm. The die block was annealed in an air annealing pit furnace. A hardness level of 195 HB over the working surface of the die was obtained. This low hardness indicates a good response to annealing, since 200–230 HB is considered to be acceptable. Prior to vacuum hardening and tempering, the die was treated as follows: holes were drilled into the die for positioning a number of surface and core work thermocouples (TS and TC). These holes were 4 mm in diameter and 5 mm deep (sub-surface) and 170 mm deep (core), aluminium pick-up and oxide scale were removed from the die surface by wet blasting. These two thermocouples were used to control the heat treatment cycle and, in particular during the quenching stage, since they provide information for the direction of the quenching gas and the temperature of the die.

The heat treatment process has been followed according to the published guidelines [8,9], for heat treatment of H13 die steel, where a satisfactory microstructure (containing no pearlite and minimal pro-eutectoid carbides) can be achieved by quenching H13 steel to below 700 °C in less than 20 minutes. Further the die steel suppliers (Udderholm) recommend that a satisfactory microstructure can be achieved when cooled through the temperature range 800 °C to 500 °C in less than 20 minutes. The following two stage heating cycle (depicted in Fig. 2) was carried out:

Heating stage. Two-bar convection heating was employed up to 860 °C. It can be seen that the die was heated at a low ramp rate of 5 $°C \cdot minute^{-1}$ and held at this preheating temperatures until the core and surface temperatures were within 30 °C. The ramp rate was then reduced to 3 $°C \cdot minute^{-1}$ from 860 °C to the austenitising temperature of 1020 °C. This relatively low ramp rate was required to minimise the thermal gradient between the core and the surface. The die was held at this austenitising temperature of 1020 °C for about 30 minutes. This was measured from the point at which the die core temperature reached 1020 °C. The total heating stage was 8 hours.

Quenching stage. For this purpose the isothermal hold temperature was set at 370 °C with the quenching pressure initially set at 4 bar absolute and reduced to 2 bar pressure close to the isothermal hold set-point.

Referring to Fig. 2, it can be seen that the surface thermocouple, positioned 4 mm below the die surface, recorded 1 minute to quench to 700 °C and 3 minutes to quench through the temperature range 800 °C to 500 °C. The core thermocouple, positioned 170 mm below the surface of the 350 mm thick section die, recorded 25 minutes to quench to 700 °C and 45 minutes to quench through the temperature range 800 °C to 500 °C.

3. Numerical modelling

In this study, the computational fluid dynamics package *CFX* [10] (develops and licenses software for fluid flow analysis) is used to simulate the quenching process inside a typical vacuum heat treatment furnace. Twenty-five thousand cells were used to describe the heating chamber where large volumes of gas are directed through nozzles to impinge on the load. After the gas absorbs the heat from the hot load, a recirculation fan is designed to direct the gas back to the nozzle through the heat exchanger. In this paper our aim is to investigate the affect of various parameters such as quenching pressure, gas velocity, impact angle and

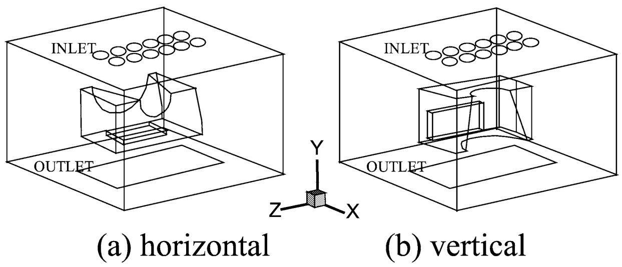

Fig. 3. Schematic diagram showing the hot zone and gas inlet and outlet for quenching in relation to the die configuration.

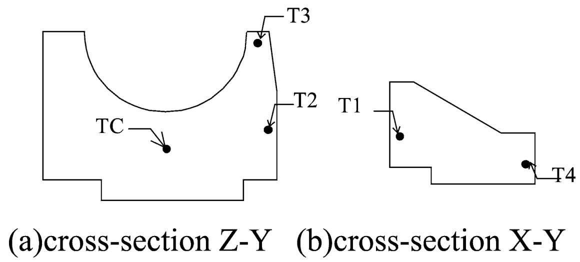

Fig. 4. Schematic diagram showing the location of points at which temperatures were monitored in the simulation.

load configurations on the fluid flow and heat transfer inside the furnace as well as the temperature distribution within the treated load. Moreover, the predicted cooling cycle is to be validated against experimental data obtained previously [7].

4. Mathematical model of heat transfer

Governing equations. The mathematical equations for gas flow and heat transfer used by CFX-4, for high Reynolds number flow, can be described as follows;

Continuity equation

$$\frac{\partial \boldsymbol{\rho}}{\partial \boldsymbol{t}} + \nabla \bullet (\boldsymbol{\rho U}) = \mathbf{0} \tag{1}$$

Momentum equation

$$\frac{\partial \boldsymbol{\rho U}}{\partial \boldsymbol{t}} + \nabla \bullet (\boldsymbol{\rho U} \otimes \boldsymbol{U}) - \nabla \bullet (\boldsymbol{\mu}_{\mathrm{eff}} \nabla \boldsymbol{U}) = -\nabla \boldsymbol{p}' + \nabla \bullet \left(\boldsymbol{\mu}_{\mathrm{eff}} (\nabla \boldsymbol{U})^{\mathrm{T}}\right) + \boldsymbol{B} \tag{2}$$

where $\boldsymbol{\rho}$ and $\boldsymbol{U}$ are mean fluid density and velocity, p the pressure, t the time, B body force and $\boldsymbol{\mu}_{\mathrm{eff}}$ is the effective viscosity: $\boldsymbol{\mu}_{\mathrm{eff}} = \boldsymbol{\mu} + \boldsymbol{\mu_T}$ and $\boldsymbol{\mu_T}$ is the turbulent viscosity.

$$\boldsymbol{\mu_T} = \boldsymbol{C_\mu \rho} \frac{\boldsymbol{k}^2}{\boldsymbol{\varepsilon}}$$

The energy equation is

$$\frac{\partial \boldsymbol{\rho H}}{\partial \boldsymbol{t}} + \nabla \bullet (\boldsymbol{\rho U H}) - \nabla \bullet (\boldsymbol{\lambda} \nabla \boldsymbol{T}) = \frac{\partial \boldsymbol{p}}{\partial \boldsymbol{t}} \tag{3}$$

where T is the temperature, λ is the thermal conductivity and H is the total enthalpy.

Table 1
Constants used in the RNG model

C_μ	C_1	C_2	C_3	σ_k	σ_ε	β	η_0
0.085	1.42	1.68	0	0.7179	0.7179	0.015	4.38

CFX-4 solves the heat conduction equation for the temperature in the solid region as follows;

$$\frac{\partial(\boldsymbol{\rho_s H})}{\partial \boldsymbol{t}} - \nabla \bullet (\boldsymbol{\lambda_s} \cdot \nabla \boldsymbol{T}) = \mathbf{0} \tag{4}$$

where: $H = C_S T$, and ρ_s, C_s, λ_s are density, specific heat, and the thermal conductivity of the solid.

Turbulence modelling. *RNG K & ∈ turbulence model* (Re-normalization group methods) is normally recommended where complex geometry with high Reynolds number flow is being examined. The equations used to describe the turbulence model are:

$$\frac{\partial \boldsymbol{\rho k}}{\partial \boldsymbol{t}} + \nabla \bullet (\boldsymbol{\rho U k}) - \nabla \bullet \left(\left(\boldsymbol{\mu} + \frac{\boldsymbol{\mu_T}}{\boldsymbol{\sigma_k}}\right) \nabla \boldsymbol{k}\right) = \boldsymbol{P} + \boldsymbol{G} - \boldsymbol{\rho \varepsilon} \tag{5}$$

and

$$\frac{\partial \boldsymbol{\rho \varepsilon}}{\partial \boldsymbol{t}} + \nabla \bullet (\boldsymbol{\rho U \varepsilon}) - \nabla \bullet \left(\left(\boldsymbol{\mu} + \frac{\boldsymbol{\mu_T}}{\boldsymbol{\sigma_\varepsilon}}\right) \nabla \boldsymbol{\varepsilon}\right) = (\boldsymbol{C}_1 - \boldsymbol{C}_{1\mathrm{RNG}}) \frac{\boldsymbol{\varepsilon}}{\boldsymbol{k}} \big(\boldsymbol{P} + \boldsymbol{C}_3 \max(\boldsymbol{G}, \mathbf{0})\big) - \boldsymbol{C}_2 \boldsymbol{\rho} \frac{\boldsymbol{\varepsilon}^2}{\boldsymbol{k}} \tag{6}$$

Where k is turbulence kinetic energy, ε is turbulence dissipation rate and P is the shear production defined by:

$$\boldsymbol{P} = \boldsymbol{\mu}_{\mathrm{eff}} \nabla \boldsymbol{U} \cdot \left(\nabla \boldsymbol{U} + (\nabla \boldsymbol{U})^{\mathrm{T}}\right) - \frac{2}{3} \nabla \bullet \boldsymbol{U} (\boldsymbol{\mu}_{\mathrm{eff}} \nabla \bullet \boldsymbol{U} + \boldsymbol{\rho k}) \tag{7}$$

and G is production due to the body force defined by:

$$\boldsymbol{G} = \frac{\boldsymbol{\mu}_{\mathrm{eff}}}{\boldsymbol{\rho \sigma_\rho}} \boldsymbol{g} \cdot \nabla \boldsymbol{\rho} \tag{8}$$

C_1, C_2 and C_3 are model constants and $C_{1\mathrm{RNG}}$ is given through the equation:

$$\boldsymbol{C}_{1\mathrm{RNG}} = \frac{\boldsymbol{\eta}(1 - \boldsymbol{\eta}/\boldsymbol{\eta}_0)}{(1 + \boldsymbol{\beta \eta}^3)} \quad \text{and} \quad \boldsymbol{\eta} = \left(\frac{\boldsymbol{P_s}}{\boldsymbol{\mu_T}}\right)^{0.5} \frac{\boldsymbol{k}}{\boldsymbol{\varepsilon}} \tag{9}$$

where η_0 and β are additional model constants, and P_s is the shear part of the production, that is the first term in Eq. (7).

Boundary and initial conditions. At the walls which occur on the domain boundary adjacent to fluid cells the velocity, the heat flux (adiabatic) and the flux of other transported scalars (e.g., mass fractions, volume fractions etc.) are considered to be zero. At the nozzle exit a constant gas velocity (Nitrogen) is assumed, which is treated as a mass source term with a corresponding source term in the axial momentum equation. The gas inlet through the top twelve nozzles is modeled with a temperature of 27 °C, pressure of

1 bar and velocity of 50 m·s^{-1}. The gas is then leaves from the domain through rectangular cross section at the bottom of the domain. The load is considered to be conduction solid with physical properties of H13 at 1030 °C as initial temperature.

5. Numerical modelling results and discussion

Figs. 5(a) and (b) show the predicted gas velocities inside the hot zone for the die in the horizontal configuration. The gas is injected directly into the hot zone at a pressure of 1 bar and an initial velocity of 50 m·s^{-1}. The X–Y cross-section shown in Fig. 5(a) indicates that as the gas impinges on the die, it spreads towards the side-walls of the hot zone creating areas of gas recirculation close to the side surfaces of the die. Furthermore, the gas velocity drops sharply from 13 m·s^{-1}, nearer to the top surface of the die to about 1 m·s^{-1} nearer to the bottom surface of the die. The gas nozzles operating outside the dimensions of the die direct the gas downwards, creating a large areas of gas recirculation at the front and back walls of the hot zone as shown in Fig. 5(b). Fig. 6 shows the temperature contours inside the die after thirty minutes. It is evident that there are variations in the temperature distribution from the surface to the core in X–Y, Z–Y and X–Z planes. This may be attributed to the flow behaviour around the die and the fact that the simulation of the flow is exclusively from the top of the hot zone.

Fig. 7 shows the cooling curves for four monitored points inside the die. The monitored point TC at the centre of the block attains 520 °C after 60 minutes of cooling. Point T1 is the next lower cooling rate, which is probably as a result of the small pocket of gas re-circulation adjacent to the die surface as shown in Fig. 5(a). Point T2 comes next where better gas flow around the surface is predicted as shown in Fig. 5(b). T3 exhibits the highest cooling rate where heat transfer from the surface occurs as a result of the direct impingement of the cooling gas on the surface.

Figs. 8(a) and (b) show the gas velocities inside the hot zone for the die in the vertical configuration. It is evident that there is a smoother gas flow around the die in a vertical configuration compared to a horizontal configuration. However, some gas recirculation also generated from the gas nozzles extending beyond the dimensions of the die as shown in Fig. 8(b). Fig. 9 shows the temperature contours inside the die in the vertical configuration after thirty minutes. It is notable that there is a relatively uniform temperature variation between the surface and the core in all-planar cross-sections (X–Y, Z–Y and X–Z). This is an interesting result, which suggests that one can achieve relatively uniform temperature profiles within the die notwithstanding the fact that the simulation of the gas flow is from the top of the hot zone.

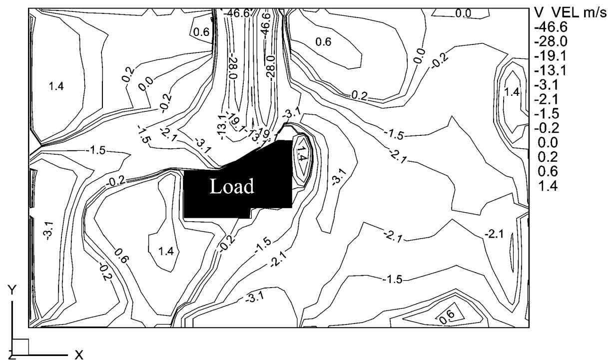

(a)

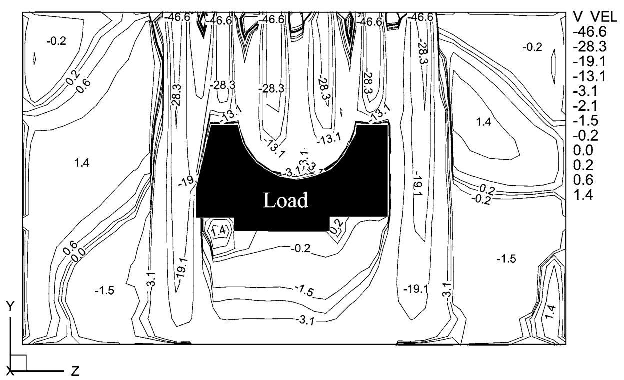

(b)

Fig. 5. (a) Gas velocity contours predicted inside the hot zone in the horizontal configuration planar cross-section X–Y. (b) Gas velocity contours predicted inside the hot zone in the horizontal configuration planar cross-section Z–Y.

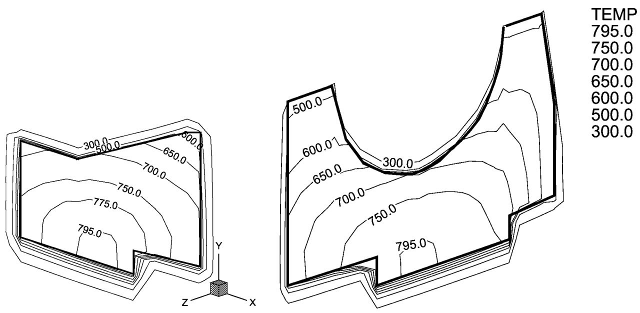

Fig. 6. Temperature contours predicted inside the die in the horizontal configuration at 30 minutes.

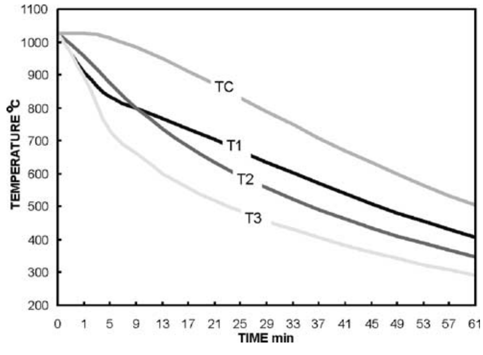

Fig. 7. Cooling curves for the monitored points inside the die in the horizontal configuration.

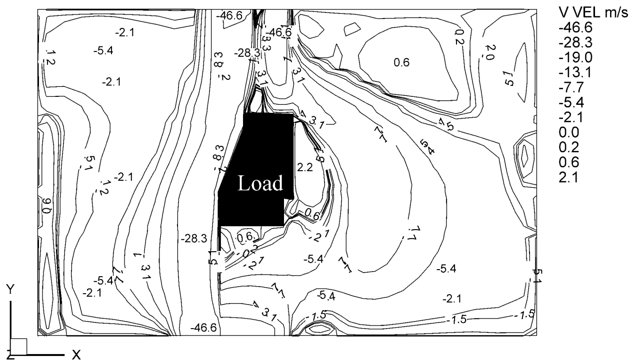

(a)

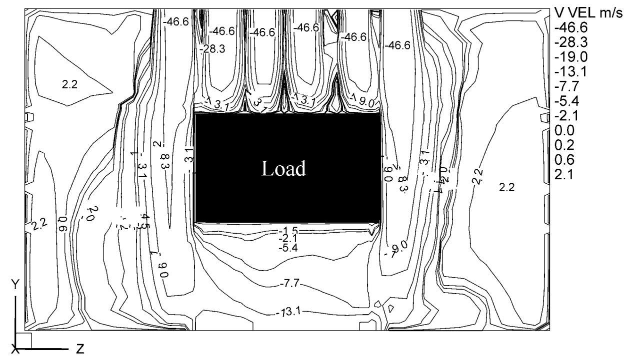

(b)

Fig. 8. (a) Simulation showing the gas velocity contours predicted inside the hot zone in the vertical configuration-planar cross-section X–Y. (b) Simulation showing gas velocity contours predicted inside the hot zone in the vertical configuration-planar cross-section Z–Y.

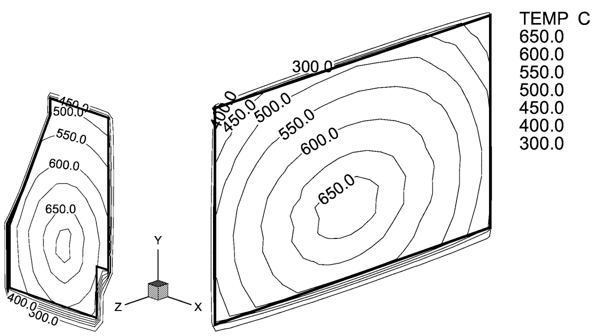

Fig. 9. Temperature contours predicted inside the treated die in the vertical configuration after 30 minutes of quenching.

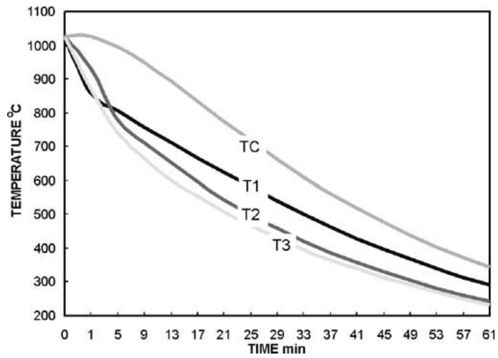

Fig. 10. Cooling curves predicted by simulation for the treated die in the vertical configuration.

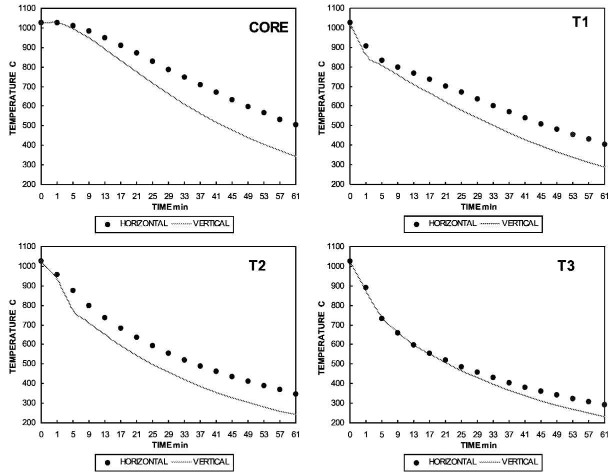

Fig. 11. Comparison between the cooling curves predicted by simulation for the heat treated die in vertical and horizontal configuration.

Fig. 10 shows the cooling curves for the monitored points inside the treated die in the vertical configuration. It is evident that there is less temperature difference between the core and the surface after 60 minutes of quenching. Fig. 11 shows a comparison between the cooling cycles for the vertical and horizontal configurations. This shows that after sixty minutes of direct quenching the points T1 and T2 in the vertical die configuration are 110 °C cooler than that of horizontal die configuration. This temperature difference increased to 160 °C toward the core of the treated die. Similar surface temperatures were also observed for the monitored point T3.

In an attempt to improve the gas velocity distribution it is possible, with the type of vacuum furnace under investigation, by oscillating the gas nozzles. In the present study, a simulation was carried out with the gas nozzles oscillating through ±30°. The effect of such oscillation was found to have little or no effect on the cooling rate inside the treated die in the vertical configuration as shown in Fig. 12. Furthermore, the effect of converting the inlet gas from the top to the bottom hot zone on the cooling rate of the die in the vertical configuration was investigated. As shown in Fig. 13, apart from the surface facing the nozzles (T1 and T4), similar cooling rates inside the die were predicted (TC and T2).

Further, simulation was carried out to study the effect of using various quenching pressures on the gas flow and resultant temperature distribution inside the hot zone. Similar gas flow behaviour around the treated die was predicted. However, by increasing the operating pressure a significant effect on the cooling rate is predicted as shown in Fig. 14.

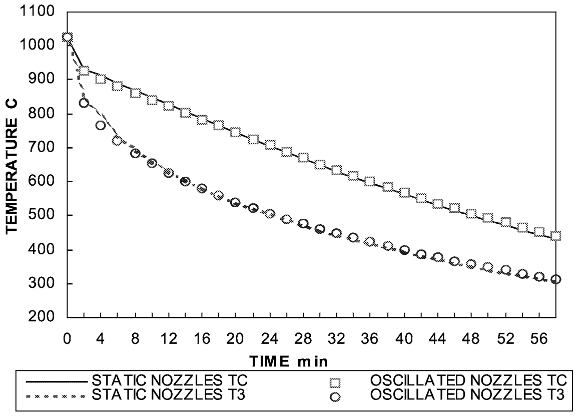

Fig. 12. Comparison of the cooling curves predicted by simulation of the die in the vertical configuration under static and oscillating gas nozzles for two monitored points TC and T3.

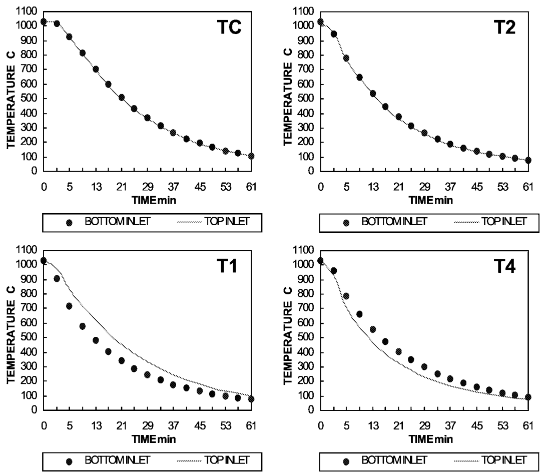

Fig. 13. Comparison of cooling curves predicted by simulation of the heat treated die in the vertical configuration with top and bottom gas quenching.

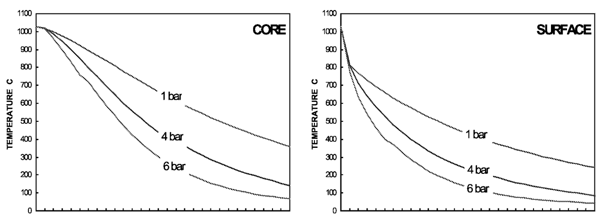

Fig. 14. Cooling curves predicted by simulation of the die in vertical configuration and under different quenching pressures.

6. Numerical simulation and validation of marquenching

Marquenching consists of quenching of the die in hot bath and holding it in the quenching medium under isothermal condition at 370 °C until the temperature of the work piece is essentially uniform. This is done only to minimise the distortion, which occurs from unequal transformation rates normally found in conventional quenching.

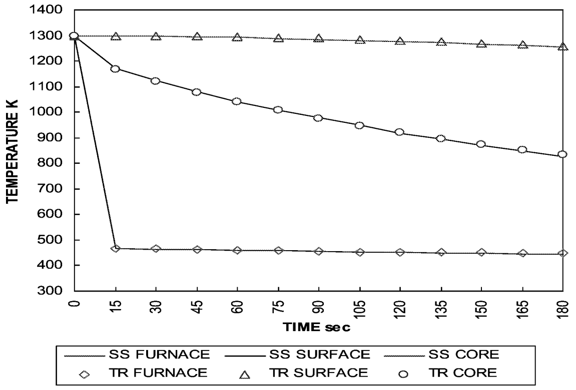

Fig. 15. Comparison of the cooling curves predicted under steady and transient flows.

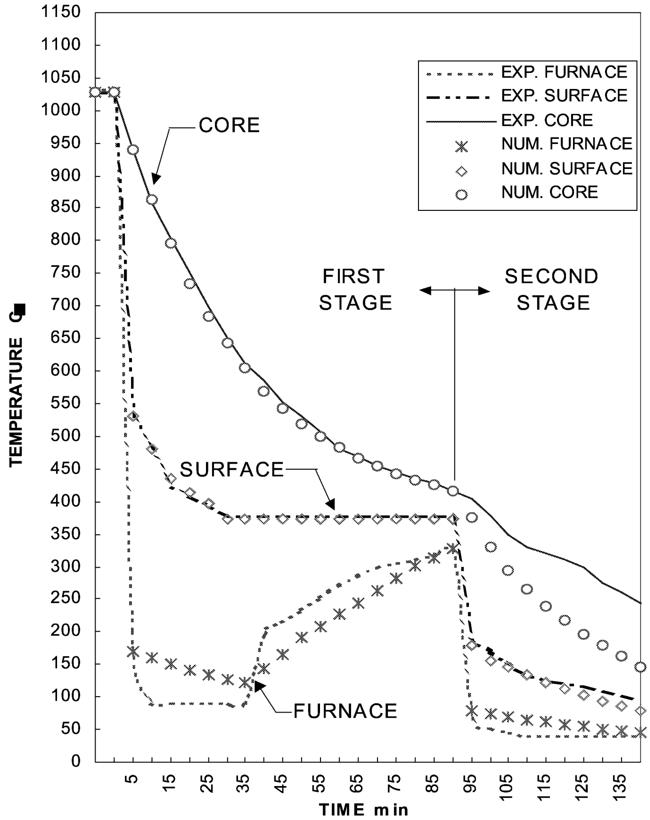

Fig. 16. Graph showing a comparison between the experimental data and numerical prediction during the marquenching process.

A three-dimensional computational model was developed to simulate marquenching of the die as operated in the plant [7]. For this process a 60 m·s^{-1} a gas velocity at quenching pressure of 4 bar were used as inlet condition. It should be also noted that the total time taken to generate the transient solution was approximately four weeks compared to four days required for the steady state solutions. In order to reduce the computational time, the numerical simulation was carried out under steady state conditions where the effect of the transient flow on the cooling rate for the first 3 minutes is minimum as shown in Fig. 15. Based on the gas velocity distributions predicted, a transient study was carried out to calculate the temperature distribution inside the die at different stages of the quenching process.

Fig. 16 shows the comparison between the numerical and experimental data. It can be seen that during the first stage of quenching, the surface temperature records 1.3 minutes to quench to 700 °C and 3 minutes to quench to 550 °C. The core reached 700 °C in 24 minutes and 550 °C in 43 minutes. The isothermal hold was set at 370 °C with the quench pressure reduced to 2 bar close to the isothermal hold set point. The second stage of quenching starts when the core temperature is within 58 °C of the die surface temperature.

As shown in the first stage of quenching for surface and core temperatures, a very close agreement is evident between the numerical simulation and the experimental data. For the second stage of quenching, both the numerical simulation and the experimental data are in reasonable agreement only for the surface temperature. The numerical simulation predicts a faster cooling rate for the core when compared to the experimental data. Currently, studies are being carried out to simulate the marquenching process based on the transient flow behaviour (developed inside the hot zone) with the nozzles oscillating during quenching.

7. Conclusion

The computational fluid dynamics package namely CFX-4 can give important insights to the gas flow inside the hot zone and temperature profiles generated in large dies during quenching. It was found that transient flow simulation results fit well with both experimental and simulation results carried out for steady state flow. This numerical modelling approach indicates that the steady state flow model can be used in place of the transient flow model. Steady state simulation is an effective and efficient way to achieve satisfactory data as well as to reduce computation time and save computing resources. For the large die block modelled in this study, oscillating the gas nozzles or alternating the gas quenching from the top and bottom of the hot zone was found to have surprisingly little influence on thermal gradients within the die. Finally, a reasonably close agreement was obtained for cooling curves determined experimentally for marquenching with those predicted by numerical simulation.

Acknowledgements

The authors acknowledge and thank the support of Business Victoria, Nissan Casting Australia, Surface Technology Coatings and Mr. P. Jacques.

References

[1] J. Rodic, A. Rodic, Computer aided heat treatment and predicting of properties, Industrial Heating 10 (1983) 36–38.
[2] A. Kay, Multiflow pressure quenching in vacuum furnaces, Vacuum 42 (17) (1991) 1103–1107.
[3] R. Arola, H. Martikeinen, J. Virta, Computer aided simulation of the temperature and distortion of components during heating up in heat treatment furnaces, Materials Science Forum 102–104 (1992) 783–790.
[4] A.K. Singh, D. Mazumdar, Mathematical modeling of thermal fields during heat treatment of steel, Steel Research 63 (5) (1992) 194–200.
[5] A. Mochida, K. Kudo, Y. Mizutani, M. Hattori, Y. Nakamura, Transient heat transfer analysis in vacuum furnaces heated by radiant tube burners, Energy Conversion and Management 38 (10–13) (1997) 1169–1176.
[6] J.H. Canybear, Vacuum hardening of H13 die steels: Experience with convective assisted heating and isothermal holding in regard to distortion and metallurgical properties, Industrial Heating 60 (8) (1993) 45–48.
[7] I. Katatny, P. Jacques, A.S. Blicblau, E.D. Doyle, Y. Morsi, Performance and computer simulation of large H13 dies in vacuum heat treatment, in: Proceedings 17th Heat Treating Society Conference, Indianapolis, ASM International, Materials Park, OH, 1997.
[8] H.P. Nicholas, Standardising H13 die casting heat treatment, in: H. Berns, et al. (Eds.), New Materials Processes Experiences for Tooling Materials, Proceedings of the International European Conference on Tooling Materials, Interlaken, 7–9 September 1992, Andelgingen, Mat. Search, 1992, pp. 450–457.
[9] North American Die Casting Association, NADCA recommended procedures for H-13 tool steel, NADCA, Rosemont Illinois, 1997, 32 p.
[10] CFX-4, AEA Technology, plc, Oxfordshire, United Kingdom, 2000.